Separation and Purification Technology 305 (2023) 122530

Contents lists available at ScienceDirect

Separation and Purification Technology

journal homepage: www.elsevier.com/locate/seppur

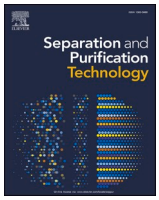

Exploring the effect of a polyacrylic acid-based grinding aid on magnetite-quartz flotation separation

Vitalis Chipakwe *, Tommy Karlkvist, Jan Rosenkranz, Saeed Chehreh Chelgani *

Minerals and Metallurgical Engineering, Department of Civil, Environmental and Natural Resources Engineering, Lulea University of Technology, SE-971 87 Lulea, Sweden

ARTICLE INFO

Keywords:
Grinding aid
Polymer
Polyacrylic acid
Flotation performance
Grinding
Pretreatment
Energy

ABSTRACT

It is well documented that the use of grinding aids (GAs) can reduce milling energy consumption. However, the impact of GAs on downstream processes must be addressed in view of complex processes such as froth flotation separation. This study investigates the effects of polyacrylic-based grinding aids (Zalta™ GR20-587: AAG) on the grinding performance and quartz flotation from magnetite. Various AAG dosages and conditions were examined. The grinding results showed lower energy consumption and a finer, more uniform product size with roughened surfaces for AAG compared to grinding without the grinding aid. Flotation tests of single pure minerals showed that AAG enhanced quartz collection with minimal effect on magnetite. Mixed mineral flotation showed that by using AAG, Fe recovery of 92.1 % and 64.5 % Fe grade could be achieved with a lower collector dosage of 100 g/t compared to 200 g/t in the absence of AAG. Zeta potentials and stability measurements showed that AAG shifts the potential, thus improving the stability and dispersion of the suspension. Adsorption tests illustrated that AAG adsorbed on both quartz and magnetite, the former having a higher capacity. FTIR indicated the physisorption interaction between AAG and the minerals. Therefore, the presence of AAG not only improved grinding efficiency but could potentially decrease the amount of collector required to achieve comparable metallurgical performance.

1. Introduction

Minerals' size reduction and liberation are associated with high energy consumption coupled with low efficiency [1–3]. Among many efforts to address these challenges, the use of grinding aids has been proposed as one of the potential solutions [4–6]. It is well documented that grinding aid (GA) can improve grinding performance, prevent agglomeration, generate narrow-size products, and reduce energy consumption [7–10]. Although understanding of the mechanism of the effect of these GAs remains unsatisfactory, there is a consensus that the adsorption of these chemical additives is a prerequisite for their applications [5,6]. It can be postulated that these chemicals will remain on the surface of the particles after milling.

Since size reduction is usually followed by the subsequent concentration or separation processes, it is paramount to ensure that the integrity and performance of these downstream processes are not compromised. Grinding as a step prior to the flotation separation process influences the surface properties of the particles, the solution/pulp chemistry, the surface chemistry, and even the crystal structure [11–15]. Ersoy et al. [16] investigated the effect of triethanolamine (TEA) and monoethyl glycol (MEG) (the most typical GAs) on the surface of calcium carbonate. Both GAs have been reported to adsorb on particle surfaces, resulting in changes in product properties, such as rheology, dispersion, and color properties [16]. Bulejko et al. [12] examined the effect of 0.1 wt% TEA in ultrafine wet grinding of corundum. TEA affected zeta potentials, turbidity, viscosity, and improved grinding performance. They considered only one TEA concentration (0.1 wt%) and reported relatively unstable suspensions based on zeta potentials and turbidity measurements [12]. Although several studies have discussed the effects of GAs on the final product (centered on the cement and aggregate industry, where grinding is usually the final step), few investigations have addressed their effects on products in view of downstream processes such as flotation [5,6]. In addition to the change in product properties during grinding, froth flotation involves using surfactants that can potentially interact with these grinding aids.

Polyacrylic acid (PAA) and its derivatives are widely used in mineral processing in different applications, as flocculants, dispersants, depressants, and viscosity modifiers [3,17–23]. Zhang et al. [21] examined

* Corresponding authors.
E-mail addresses: vitalis.chipakwe@ltu.se (V. Chipakwe), saeed.chelgani@ltu.se (S.C. Chelgani).

https://doi.org/10.1016/j.seppur.2022.122530
Received 29 August 2022; Received in revised form 10 October 2022; Accepted 29 October 2022
Available online 3 November 2022

the effect of PAA as a depressant in the flotation of calcite and fluorite. PAA was selectively adsorbed on calcite, selectively depressed, and improved fluorite recovery with sodium oleate at pH 7. Quezada et al. [24] reported that applying PAA could improve the sedimentation and storage of quartz, montmorillonite, and kaolinite flotation tailings. Through molecular dynamics simulation, PAA was reported to adsorb on quartz and clay mineral surfaces, ultimately preventing agglomeration of the tailings and allowing easy dewatering. Chen et al. [25], during the flotation separation of chalcopyrite and magnesium silicates with potassium xanthate (a collector) and gum Arabic (a depressant), found that the presence of a PAA-based polymer (sodium polyacrylate) improved the process. The synergism between sodium polyacrylate and gum Arabia allowed selective depression of magnesium silicate minerals, namely talc and serpentine. The improved flotation separation was attributed to the PAA dispersion effect in removing serpentine particles from the surface of the talc, which allowed gum Arabia to adsorb on the talc surface [25]. In size reduction units, using these GAs, such as PAA, makes it inevitable that these additives can directly or indirectly enter downstream separation processes, such as flotation. Froth flotation remains the most versatile separation technique, yet very complex, utilizing differences in natural or imparted wettability of the mineral surface [26–29]. In flotation, solution and surface chemistry are important in understanding the physicochemical processes occurring at the solid-water and the air–water interface [30,31].

GA polymers used primarily in solid–liquid separation units have been reported to enhance or depress flotation depending on their types, particle type, polymer concentration, and contact time [32]. From this detailed review of the literature, it is evident that more research is required in designing and selecting chemical additives used as GAs to ensure compatibility with the specifications of the product and downstream processes. Although some studies have been reported on polymer-surfactant interactions, mostly in flocculants, this study, as a practical approach, focuses on their interaction through GA-surfactant. This study first investigates the effect of a polyacrylic acid-based grinding aid (Zalta™ GR20-587: AAG) on the grinding performance and the surface of the ground particle. The effect of AAG on surface properties and pulp chemistry was then explored together with the resulting flotation behavior. The results of this study will aid in the development and selection of future multifunctional additives to further improve beneficiation performance.

2. Materials and methods

2.1. Materials

For the study, samples of pure quartz (99.9 % SiO_2) and magnetite (96.0 % Fe_3O_4) were obtained from VWR, Sweden (Fig. 1). For grinding experiments, a narrow particle size range of the mixture (−2.8 + 2 mm) was used as the grinding feed. The pure minerals were ground separately for flotation tests and subsequent surface analysis. From the resulting product, samples with a size fraction of −106 + 38 μm were used for flotation and adsorption tests. The −38 μm size fraction was further ground and used for subsequent surface analysis.

For all experiments, the anionic polyacrylic-based polymer (Zalta™ GR20-587: AAG) provided by Solenis with a typical chemical structure shown in Fig. 2 was used as GA. For grinding tests, AAG was used as received (aqueous form), and no stock solution was prepared to eliminate the effect of water. A cationic ether amine collector, Lilaflot 822 M, was obtained from Nouryon, Sweden. Analytical grade corn starch used as a magnetite depressant was purchased from Merck. Analytical grade HCl and NaOH (Merck) were prepared in an appropriate solution for pH adjustments.

2.2. Grinding test

A laboratory scale ball mill (CAPCO, UK) with a 115 mm internal diameter and a total volume of 1.4 L was used for the grinding experiments. The total grinding time of 30 min and the set parameters (19 vol % mill filling; 0.16 w/w feed: ball ratio; 10–36 mm graded steel balls) were predetermined as optimal for dry grinding in a natural atmosphere. Optimal parameters were adopted for all tests to reduce grinding energy, study the effect of GAs, and generate material for subsequent flotation tests. In the reference (blank), no additives were added, and for the other tests, AAG was combined with ore at three levels (300, 500, and 1000 g/t). The grinding products were subjected to particle size distribution (PSD) using a particle size analyzer (Mastersizer 3000, Malvern Instruments, UK), from which P_{80}, X_{10}, X_{50}, and X_{90} were determined. For a better assessment of the particle size distribution, the uniformity of the product was calculated using Eq. (1), which is a measure of the PSD

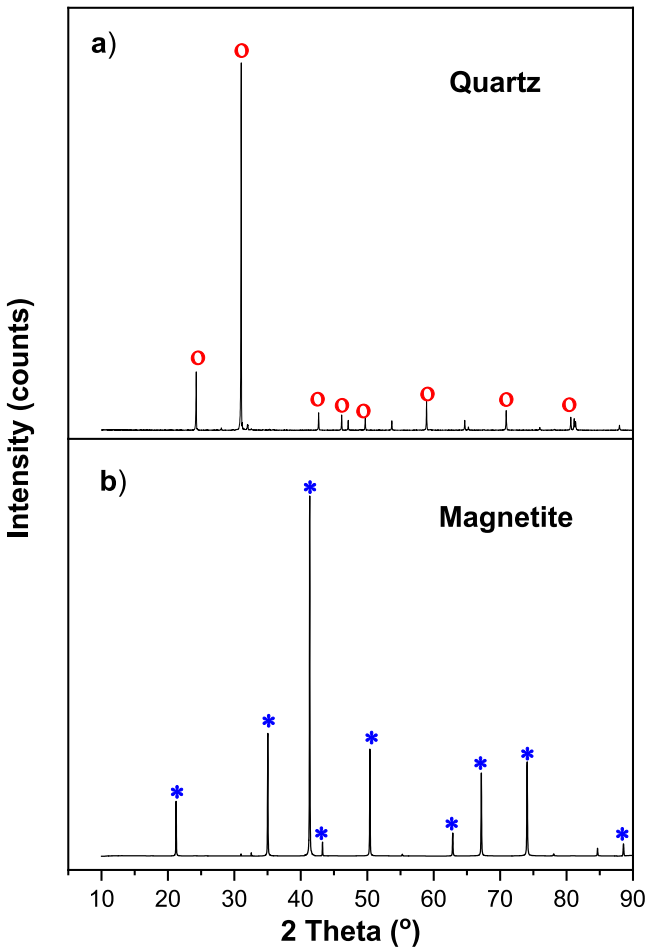

Fig. 1. XRD pattern for (a) pure quartz and (b) pure magnetite.

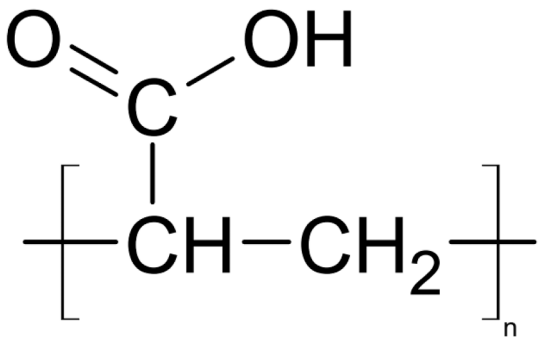

Fig. 2. Chemical structure of typical polyacrylic acid.

span. The smaller the value, the narrower the PSD [33,34].

$$Uniformity[-] = \frac{X_{90} - X_{10}}{X_{50}} \quad (1)$$

Here, X_{10}, X_{50}, and X_{90} are the diameters corresponding to 10, 50, and 90 vol% on a relative cumulative particle size distribution curve. Energy consumption was characterized using the work index according to the Bond equation (Eq. (2)) [35]. Where: Wi: work index (kWh/t), W: grinding energy (kWh/t), P: 80 % passing size of the mill product, in μm, F: 80 % passing size of the mill feed, in μm. The same grinding protocol was used for single minerals and the artificial mixture (magnetite: quartz 2:1). After grinding and wet sieving, the samples were thoroughly washed with a 2 % HCl solution to eliminate possible contamination the mineral surfaces.

$$W = 10.W_i\left(\frac{1}{\sqrt{P}} - \frac{1}{\sqrt{F}}\right) \quad (2)$$

2.3. Surface area and morphology

A sample was taken from the ground product for the surface area and morphology study. A Micromeritics Flowsorb II 2300 instrument was used to measure surface area based on the BET (Brunner Emmet Teller) method. Further, the surface roughness (R_S) was calculated using Eq. (3) [36].

$$R_S = A_B\rho\left(\frac{D}{6}\right) \quad (3)$$

where A_B is the BET surface area (m^2/g), ρ is the density of the sample, and D is the average particle diameter. Surface morphology under different grinding conditions was characterized by scanning electron microscopy (SEM). Secondary imaging (SE) was performed using the Zeiss Sigma 300 VP instrument (QanTmin).

2.4. Flotation test

Quartz and magnetite flotation tests were carried out using a 150 ml mini flotation cell (Clausthal cell, Germany) operated at 310 rpm and an airflow rate of 2 L/min. 7.5 g of the sample was added to the flotation cell with deionized water for each test. Before the flotation stage, the pulp was agitated with the required amount of AAG for 10 min to allow adsorption on the particle's surface. The required amount of depressant and collector was added to the pulp together with the corresponding pH adjustments for 10 min. An alkaline starch solution was prepared as a depressant together with Lilaflot 822 M as a collector. The total flotation time was 2 min, and afterward, the floats and sinks were collected, filtered, weighed, assayed, and recovery was calculated. In addition to single-pure mineral flotation, experiments were also carried out on the magnetite-quartz artificial mixture (at a 2:1 ratio). The selectivity S was calculated using equation (4) to assess the flotation performance under varying conditions. Where R_1 is the recovery of magnetite and R_2 is the recovery of quartz. A higher selectivity index S extrapolates better selectivity for the flotation separation [37,38].

$$S = R_1 - R_2 \quad (4)$$

2.5. Zeta potential measurements

The zeta potential measurements were carried out using the CAD ZetaCompact instrument (CAD Instruments, France). For the measurements, 20 mg of each mineral sample (−5 μm) was dispersed in 50 ml of potassium chloride solution (background electrolyte) together with predetermined reagents. The required pH adjustments were made using 0.1 M NaOH or HCl. Measurements were done in triplicate, and the average was reported.

2.6. Stability measurements

Stability measurements of the suspension were done using a turbidimeter (Turbiscan LAB Expert, Formulaction, France). The suspension (50 mg sample in 40 ml water) was mixed with varying reagent concentrations. Measurements were made using 20 ml aliquots and scanned at the height of 40 mm at 30° C. The measurements were conducted for 60 min at 30-second intervals. The light transmission and backscattering data obtained were used to calculate the Turbiscan stability index (TSI) (Eq. (5)). The values of the TSI coefficient range from 0 to 100 where the lower the stability of the value, the higher the suspension [22,39].

$$TSI = \sqrt{\frac{\sum_{i=1}^{n}(x_i - X_{BS})^2}{n-1}} \quad (5)$$

where x_i is the average backscattering for a measurement per minute, x_{BS} is the average x_i, and n is the number of scans.

2.7. Adsorption measurements

The adsorption of AAG on quartz and magnetite was measured using an ultra-violet visible spectrometer (DU Series 730 – Beckman Coulter, USA) at wavelength 210 nm in triplicate. For magnetite and quartz, 1.0 g particles were mixed with predetermined reagents at pH 10 in a 100 ml flask. To maximize adsorption, the mixture was stirred for 2 h. The adsorption capacity was calculated based on the depletion method using equation (6);

$$Q_e = \frac{(C_1 - C_0)V}{m} \quad (6)$$

where Q_e represents the adsorbed AAG on the sample particle surface in mg/g, C_0 and C_1 are the initial and residual AAG concentrations in mg/L, whilst V and m are AAG solution volume (L) and mass of mineral sample (g), respectively. The experimental data of the adsorption isotherm were fitted to the Langmuir (Eq. (7)), and Freundlich models (Eq. (8)) models, and the curve parameters are summarized in Table 4.

$$Q_e = \frac{K_L C_e Q_0}{1 + K_L C_e} \quad (7)$$

$$Q_e = K_F C_e^{\frac{1}{n}} \quad (8)$$

where Q_e represents the amount of AAG (mg/g) adsorbed, C_e is the concentration of AAG at equilibrium. From Langmuir and Freundlich equations, the constants Q_m and K_L and K_F and $1/n$ respectively relate to the maximum adsorption capacity and the adsorption energy, respectively [40].

2.8. FT-IR measurements

FTIR spectra were obtained using an IFS 66 V/S instrument and a Vertex 80v instrument for diffuse reflectance (DR) and attenuated total reflectance (ATR), respectively (Bruker Optics, Ettlingen, Germany). For conditioning, 2.0 g pure samples were mixed with predetermined reagents (100 mg/L AAG and 50 mg/L Lilaflot 822 M) and conditioned for 40 min at pH 10. The solid samples were thoroughly washed with deionized water and dried at 35 °C for 24 h. The samples were mixed with potassium bromide. The scanning range was 400–4000 cm^{-1} at a resolution of 4 cm^{-1}.

3. Results and discussion

3.1. Grinding performance

To determine the optimal dose of GA to improve grinding perfor-

mance, a series of experiments using AAG were conducted. Grinding performance was first evaluated based on energy consumption (Ec) relative to the reference test (without AAG). The introduction of AAG decreases Ec to give a minimum of 16.69 kWh/t at 500 g/t compared to 19.41 kWh/t as reference (Table 1). Further the d_{80} of the product showed that 500 g/t is the optimal dosage with 184 μm whilst the reference had 207 μm (Table 1). The positive effect of grinding aids on improving product fineness has been observed in the literature [10,41–43]. The improvement in fineness points to better grinding due to improved material flowability resulting from the reduction in agglomeration [5,6,41,44,45]. In terms of uniformity, which generally measures PSD, the introduction of AAG results in a narrow PSD width (lower number uniformity). Furthermore, the specific surface area increases with the addition of AAG, with the highest of 0.6510 m^2/g at 500 g/t together with a corresponding maximum roughness of 0.3180 compared to 0.2389 for the reference (Table 1). The superior surface area result of the application of grinding aids compared to blank conditions has been widely reported in the literature [17,19]. Liu et al. 2021 [17], during cobalt aluminate using sodium polyacrylate, the specific surface area was greater (39.56 m^2/g) compared to the blank condition (20.18 m^2/g). In summary, the addition of an optimum amount of AAG improves the grinding performance evident from the reduction in Ec, the generation of new surfaces (higher SSA), and improved uniformity of the particles.

3.2. Surface morphology of ground products

Given downstream separation processes, the grinding stage goes beyond size reduction, as it involves a change in particle properties such as shape, roughness, and physicochemical properties [14,15]. These morphological characteristics have been shown to influence flotation performance [14,15,46]. SEM images were provided and analyzed to further characterize the effect of AAG on the morphological characteristic. Fig. 3 shows differences in the particle surface of the reference ground sample (Fig. 3a) compared to the ground in the presence of AAG at 1000 g/t (Fig. 3b), with the latter showing roughening of the surfaces. The reference particle shows smoother surfaces with some fragmented smaller particles on the surface. Smaller particles on the surface suggest an interparticle attraction that points to agglomeration tendencies in the absence of AAG. Similar findings have been reported in [41] on the effect of different grinding aids on fine dry grinding of calcite. SEM analysis of ground samples showed more agglomerates in the blank compared to particles with grinding aids [41]. Grinding mechanisms, such as abrasion and impact, have been reported to influence particle shape and roughness [14,47]. The observed roughening for AAG is consistent with the calculated roughness and the measured SSA, which is superior to the reference. The observed roughening could be attributed to the reduced contribution of abrasion due to the improved flowability with the introduction of AAG. Looking closely at the zoomed-out images, AAG generally resulted in a more uniform and overall finer particle size distribution than the reference, consistent with the findings from the Mastersizer particle analyzer.

Table 1
Effect of AAG on grinding performance and product (Ec expressed as work index).

Conditions	Ec (kWh/t)	D_{80} (μm)	Uniformity (–)	SSA (m^2/g)	Roughness (–)
Reference	19.41	207	2.056	0.4891	0.2389
300 g/t	17.28	187	1.848	0.5857	0.2861
500 g/t	16.69	184	1.797	0.6510	0.3180
1000 g/t	17.80	192	1.813	0.5628	0.2749

Table 2
Summary of the adsorption parameters of AAG on quartz and magnetite.

Mineral	Langmuir			Freundlich		
	Q_m	K_L	R^2	n	K_F	R^2
Quartz	3.45	0.718	0.9711	5.20	1.70	0.8851
Magnetite	3.19	0.315	0.9701	4.72	1.33	0.8365

3.3. Single mineral flotation

The flotation experiments were carried out on single minerals to study the effect of AAG in the ether-amine system (Lilaflot 822 M) for quartz and magnetite at pH 10 (Fig. 4a). The results demonstrated that by increasing the Lilaflot 822 M concentrate as a collector, both the quartz and magnetite recoveries increase, in addition to the absence or presence of AAG. Further analyses reveal that the addition of AAG increases the floatability of quartz and magnetite (Fig. 4a). The observed increase in the floatability of quartz in the presence of Lilaflot 822 M (an ether amine) corroborates with the literature findings showing amine's efficacy at pH 10 [48,49]. Quartz recovery reached a maximum of 90 % at 20 mg/L of the collector in the absence of AAG, while it would be 92 % at 10 mg/L of the collector in the presence of AAG. In other words, higher recoveries were achieved in the presence of AAG at a lower collector concentration. Similar behavior is observed for magnetite floatability, which at 20 mg/L collectors, its recovery increases from 15 to 80 % in the absence and presence of AAG, respectively. Generally, in both scenarios, the presence of AAG enhances the floatability of both quartz and magnetite.

In addition to the system, the effect of AAG on the floatability of quartz and magnetite in the presence of a depressant was investigated. Starch was utilized as a depressant to address the undesirable floatability of magnetite in the reverse flotation setup. The floatability was investigated at different starch concentrations at a fixed collector dosage of 20 mg/L and pH 10. As expected, a minimum effect was observed on quartz floatability with some decreases at concentrations above 80 mg/L (Fig. 4b). For the reference sample, starch was effective in depressing magnetite, giving the lowest floatability of 3 % at 50 mg/L starch concentration. In the presence of AAG, magnetite floatability was found to be quite high, with the lowest floatability of 2 % achieved only at 100 mg/L starch concentration. Evidently, the presence of AAG results in increased starch dosages. The single mineral flotation test showed that the application of AAG improved the collection of quartz and magnetite even at a lower collector dose. However, it was also observed that the addition of AAG increases the amount of depressant to counter the improved collection of magnetite. To gain a complete understanding of the behaviors observed in single mineral flotation, artificial mixtures were used in subsequent flotation tests.

3.4. Flotation of artificial mixture

Flotation tests on the artificial mixture were performed on the magnetite and quartz mixture with a mass ratio of 2:1 to determine the effect of improved quartz collection separation from magnetite. The flotation feed of the mixture had a Fe grade of 58.7 %. As shown in Fig. 5, the addition of AAG influences both recovery and grade. The result of the reference sample test shows that the recovery initially increases with increasing collector concentration to a maximum of 93.3 % at 200 g/t, after which it starts to decrease. Adding AAG improves recovery, especially at lower collector doses, supporting the findings from single-mineral flotation. At 500 g/t of AAG, a comparable maximum recovery of 92.1 % is achieved at a collector dose of 100 g/t. Adding AAG to all investigated collector concentrations, less than 200 g/t, results in higher recoveries than the reference sample. Fig. 5b agrees with the findings on the grades that increase with increasing collector and AAG concentrations. As in reverse flotation, the observed increase in

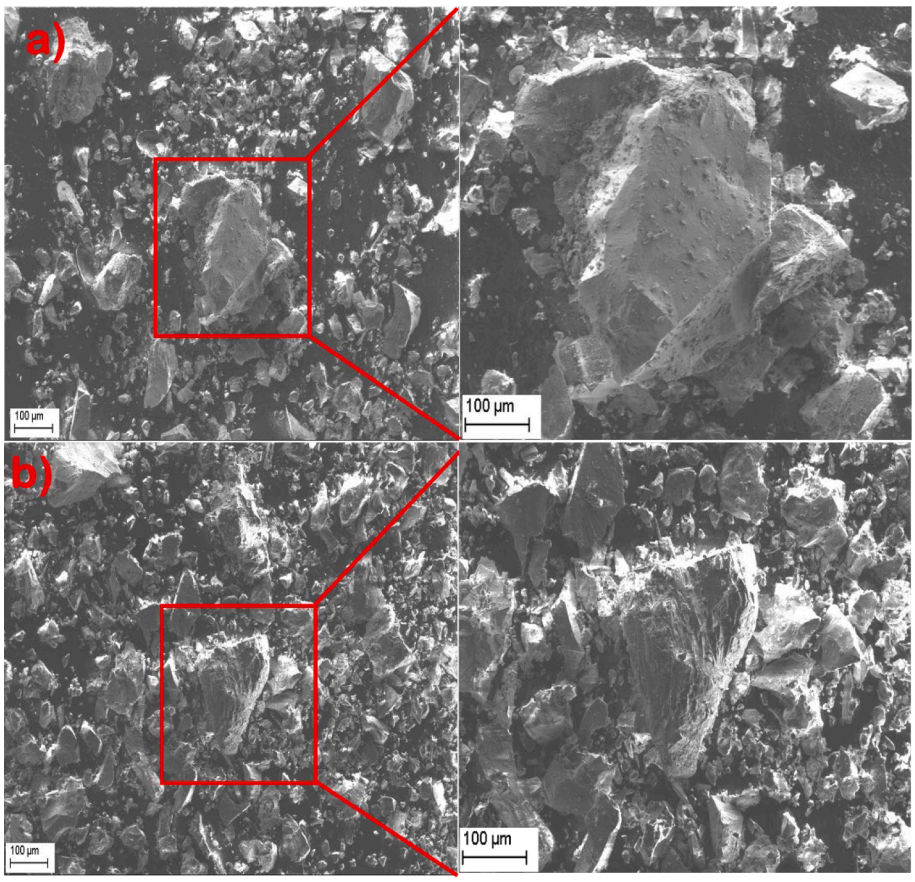

Fig. 3. SEM images showing the effect of AAG on the ground product (a) without AAG, (b) added 1000 g/t AAG.

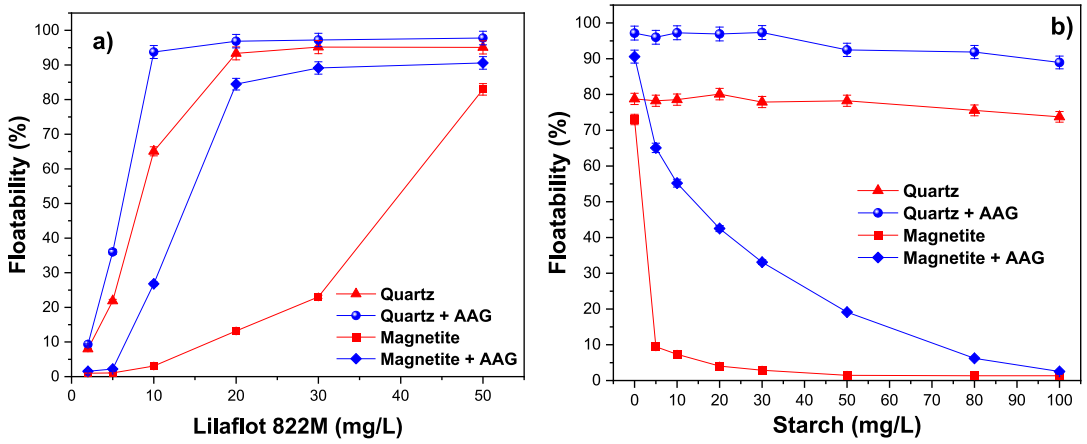

Fig. 4. Effect of AAG (100 mg/L) on magnetite and quartz single mineral flotation at pH 10 with varying (a) collector dosage and (b) depressant dosage (fixed collector – 20 mg/L).

grade is accompanied by a decrease in mass recovery, thus ultimately decreasing the metallurgical recovery.

Further evaluation of the selectivity of the process based on Eq. (4) is presented in Fig. 6. It can be observed that at lower collector dosages (below 300 g/t) the presence of AAG increases the process selectivity. However, it must be noted that above 300 g/t collector, the presence of AAG becomes detrimental to the process selectivity. For all scenarios, the best selectivity is reported between 200 and 300 g/t collector with a maximum of 76.2 % at 300 g/t AAG and 200 g/t collector. The results indicate that AAG enhances the collection of quartz and, to a lesser extent, the collection of magnetite. The selectivity variations at different AAG and collector dosages suggest synergistic interactions in the system. To better assess the observed effect of AAG on the separation of quartz from magnetite, surface analysis of the mineral surfaces was considered.

3.5. *Zeta potential measurements*

The effect of AAG on the colloidal stability of quartz and magnetite particles was carried out using zeta potentials from electrophoresis measurements. The change in zeta potential with varying AAG dosage at a fixed pH of 10 and 20 mg/L Lilaflot 822 M is presented in Fig. 7. For all conditions, it can be observed that the zeta potentials decreased (to a

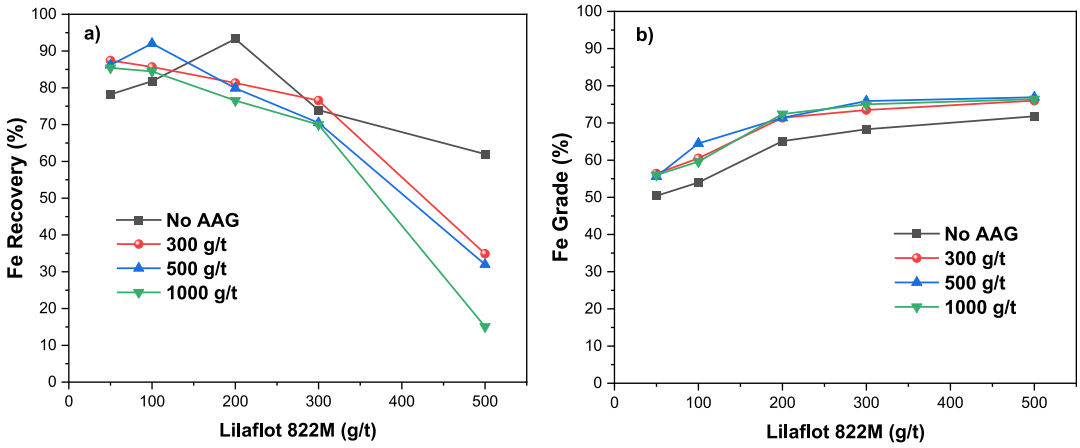

Fig. 5. Synergistic effect of AAG and collector on mixed mineral flotation (a) Fe recovery and (b) Fe grade.

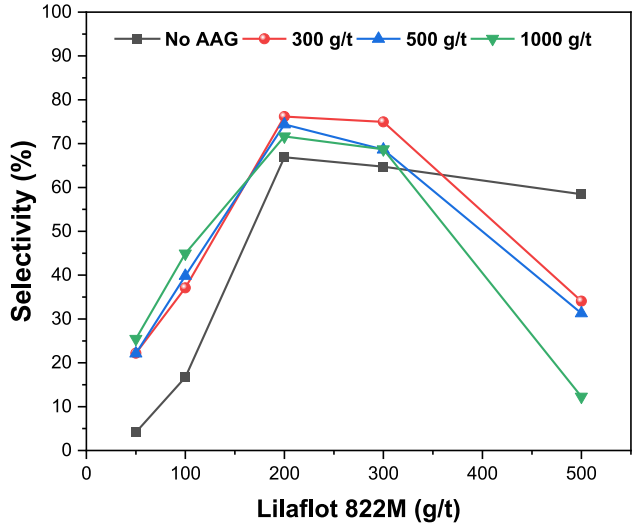

Fig. 6. Effect of AAG on selectivity with varying collector concentration.

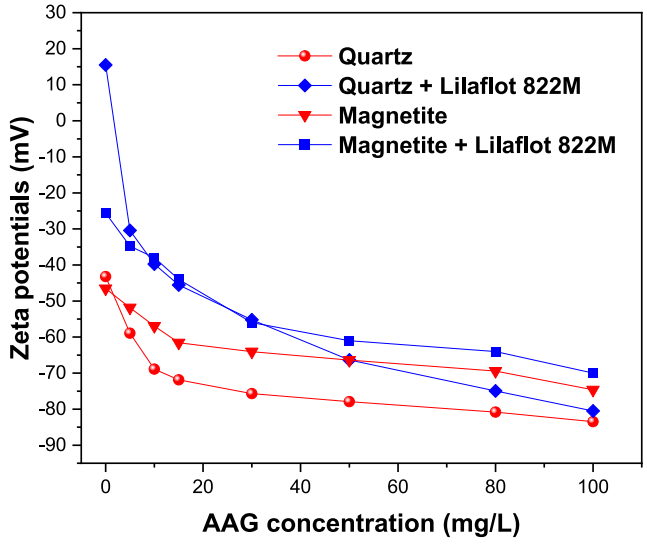

Fig. 7. Variation of zeta potentials at different concentrations of AAG at pH 10.

greater negative magnitude) when the AAG concentration was increased. For the reference test, quartz and magnetite have zeta potentials of −43.2 and −46.5 mV compared to −83.5 and −74.6 mV at 100 mg/L. The trend shows that the presence of AAG enhances the stability of the suspension regardless of the type of mineral. A similar shift in the zeta potentials is observed for both minerals as Lilaflot 822 M (a collector); however, the results show a more pronounced change for quartz, indicating increased adsorption of Lilaflot 822 M as a collector on its surface. From these observations, it could be considered that adding AAG results in an increased negative charge, especially on quartz, which could promote the interaction with the collector and improve its floatability.

3.6. Suspension stability measurements

To further understand the effect of AAG on mineral suspensions, stability studies were conducted based on the Turbiscan stability index. The variation in the Turbiscan stability index as a function of time with 100 mg/L AAG and pH 10 in quartz and magnetite suspensions is presented in Fig. 8. Similar behavior can be observed as the presence of AAG stabilizes the suspension (reduction in TSI), which corroborates the findings from the zeta potentials. The change is more pronounced for quartz than for magnetite surfaces. These findings corroborate the claim in the literature that PAA-derived polymers impart stability as a dispersant [50]. The observed decrease in stability also points to

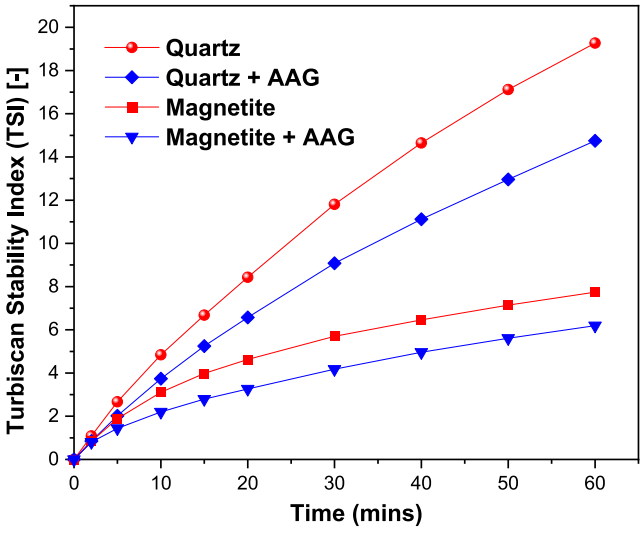

Fig. 8. Suspension stability of magnetite and quartz with and without AAG.

increased dispersibility with the introduction of AAG, which can also increase the quartz recovery.

3.7. Adsorption measurements

The flotation and suspension stability results showed a pronounced effect of AAG on quartz relative to magnetite. To better understand the phenomenon, adsorption measurements were performed on both mineral surfaces after treatment with varying concentrations of AAG at pH 10. Fig. 9 shows how the amount of AAG adsorbed per unit of mass increases with the AAG concentration. It is evident that quartz has a high adsorption capacity concerning magnetite in the investigated concentration. Furthermore, data fitting using the Langmuir and Freundlich models is summarized in Table 2. From the Langmuir model, the adsorption capacity (Q_m) is higher for quartz compared to magnetite, with 3.45 and 3.19, respectively. Similarly, the Freundlich model shows stronger adsorption (n) for quartz compared to magnetite, with 5.20 and 4.72, respectively. Langmuir has the best fit of the two models with an R^2 of 0.8851 compared to 0.8365 for the Freundlich model. These findings show that AAG adsorbs on both quartz and magnetite, supporting the observed effects on the flotation behavior. The superior adsorption of AAG on quartz compared to magnetite particles further explains its pronounced effect.

3.8. FTIR spectra analysis

The adsorption results showed that AAG has stronger adsorption on quartz surfaces than on magnetite surfaces. Fourier transform infrared (FTIR) spectra were performed to better understand the adsorption mechanism. Fig. 10 shows the spectra of bare and treated pure minerals of AAG, Lilaflot 822 M. For the collector (Lilaflot 822 M), characteristic peaks emerge at 2964 cm^{-1} and 2869 cm^{-1}, which are attributed to the CH_2 stretching bond of acyclic compounds [51]. Peaks at 1587, 1467, and 653 cm^{-1} can be attributed to the bending of the NH_2 or NH bonds [51–53]. A characteristic peak is observed at 1548 cm^{-1} and 1168 cm^{-1} for AAG, possibly due to the deprotonated C═O and C—O bond, respectively, since this was at pH 10 [54]. Fig. 10a shows that the surface of the introduction of AAG on the quartz mineral has no effect, and no new functional group is generated. The presence of Lilaflot 822 M is evident, with a characteristic peak showing. The characteristic OH peak at 2964 cm^{-1} changes to 2960 cm^{-1} as observed in quartz + AAG + Lilaflot 822 M, typical for an amine system [51]. A similar effect is observed for magnetite + AAG + Lilaflot 822 M with a characteristic peak from the introduction of the collector Fig. 10b. The CH peak at 2869 cm^{-1} also shifts to 2856 cm^{-1} and 2920 cm^{-1} for quartz and magnetite, respectively, after treatment. The spectra suggest a weaker Lilaflot 822 M-magnetite interaction than the Lilaflot 822 M-quartz interaction. The absence of a characteristic peak after treatment with AAG in both minerals implies that the interaction between AAG and the minerals is not chemical and thus physical adsorption.

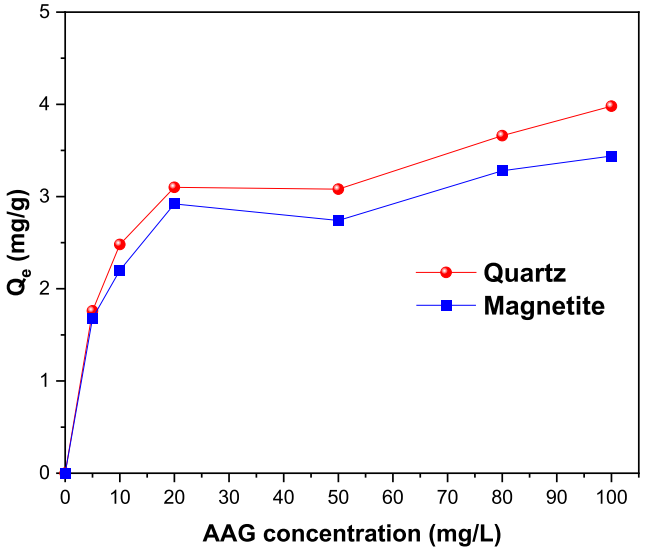

Fig. 9. Adsorption of AAG on quartz and magnetite at varying initial concentrations at pH 10.

Some interactions are evident from the observed behavior when AAG is added to both quartz and magnetite. The introduction of AAG markedly enhances the floatability of quartz with a minimal effect on magnetite. Mixed mineral flotation showed that at 500 g/t of AAG, a comparable maximum recovery of 92.1 % is achieved at a collector dose of 100 g/t. Surface analyses revealed that AAG adsorbs on mineral surfaces, increases the zeta potential (more negative), and increases the suspension stability. This is consistent with observations reported elsewhere suggesting that AAG increases dispersion and anionicity due to its anionic nature, thus increasing collector adsorption and ultimately improving flotation [32,54].

4. Conclusions

In this paper, the effect of AAG, a polyacrylic-based grinding aid, on the grinding and flotation separation behavior of a magnetite-quartz mixture was investigated. The grinding results illustrated that AAG improved the grinding efficacy at an optimum dosage and improved the product properties. The experimental results showed that the energy consumption decreased by 18 %, the specific surface area increased by 6 %, and the uniformity improved relative to the test without AAG (reference test). Further results from a single mineral flotation indicated that AAG could enhance the quartz collection, thus improving its floatability. The results of artificial mixture flotation revealed that under specific conditions of 500 g/t AAG, pH 10, 1000 g/t starch Fe recovery of 92.1 % and 64.5 % could be achieved with 100 g/t Lilaflot 822 M compared to the reference with a recovery of 93.0 % and 65.1 % grade at 200 g/t Lilaflot 822 M. The zeta potential measurement results showed a large negative shift for both quartz and magnetite; the former was more pronounced in the presence of AAG. The suspension stability results revealed that AAG results in a more stable suspension with improved dispersion compared to the reference test. The adsorption results showed superior adsorption of AAG on the quartz surface compared to magnetite. FTIR results illustrated that the adsorption mechanism of AAG on both quartz and magnetite was physical adsorption. In general, these results have addressed the long-standing question of the effect of polyacrylic-based grinding aids on the resulting products and subsequent flotation separation processes. The presence of AAG not only improved grinding efficiency but also could potentially decrease the amount of collector required to achieve comparable metallurgical performance. This paves the way for future research on the application of grinding aids in mineral processing with an approach to having grinding aids with a secondary beneficial function in view of downstream processes.

CRediT authorship contribution statement

Vitalis Chipakwe: Conceptualization, Data curation, Formal analysis, Investigation, Methodology, Visualization, Writing - original draft, Writing - review & editing. **Tommy Karlkvist:** Data curation, Supervision, Validation, Writing - review & editing. **Jan Rosenkranz:** Resources, Data curation, Supervision, Validation, Writing - review & editing. **Saeed Chehreh Chelgani:** Conceptualization, Formal analysis, Resources, Data curation, Supervision, Funding acquisition, Methodology, Visualization, Writing - original draft, Writing - review & editing.

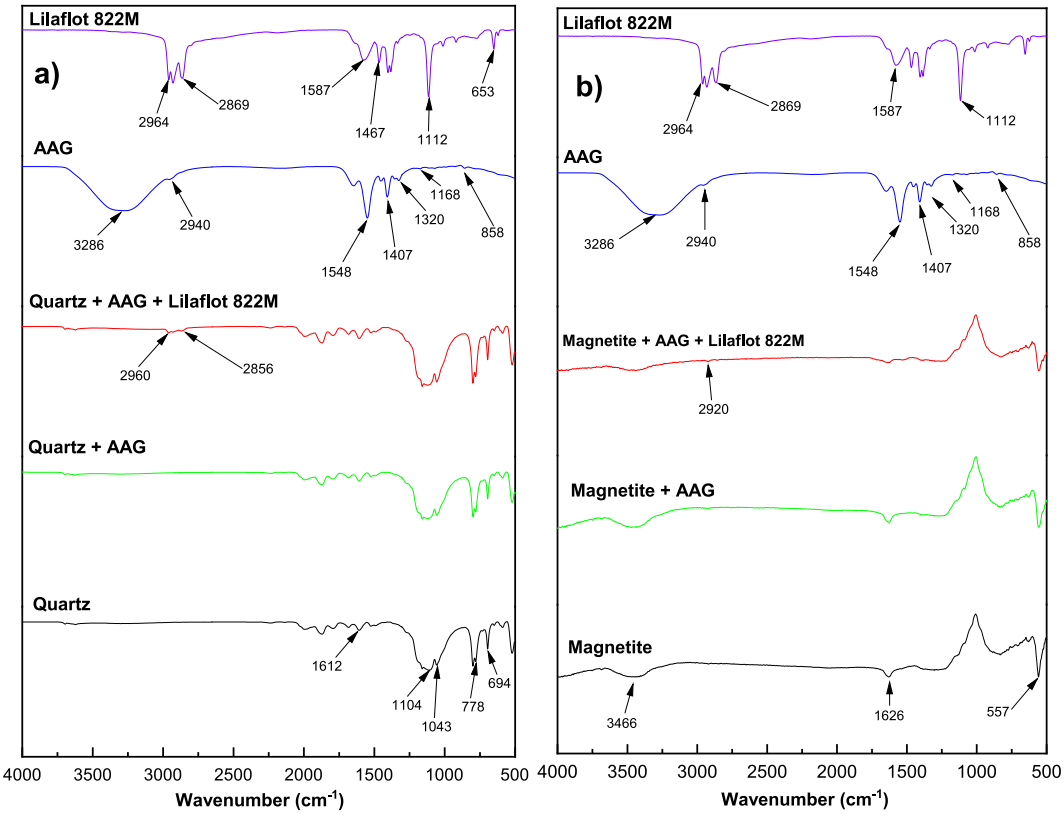

Fig. 10. FTIR spectra of AAG, Lilaflot 822 M, and bare minerals before and after treatment.

Declaration of Competing Interest

The authors declare that they have no known competing financial interests or personal relationships that could have appeared to influence the work reported in this paper.

Data availability

Data will be made available on request.

Acknowledgements

This manuscript resulted from a project financially supported by CAMM^2, the Center of Advanced Mining and Metallurgy, as a center of excellence at the Luleå University of Technology, and Vinnova for the RIO-MUN (Reverse flotation of iron oxide using magnetic, ultrasonic, nanobubble technology), project number: 2020-04835. The authors also thank Nouryon (Sweden) and Solenis for their help with the reagents used in this study.

References

[1] J. Jeswiet, A. Szekeres, Energy consumption in mining comminution, Proc. CIRP. 48 (2016) 140–145, https://doi.org/10.1016/j.procir.2016.03.250.
[2] T. Napier-Munn, Is progress in energy-efficient comminution doomed? Miner. Eng. 73 (2015) 1–6, https://doi.org/10.1016/j.mineng.2014.06.009.
[3] M. He, Y. Wang, E. Forssberg, Slurry rheology in wet ultrafine grinding of industrial minerals: a review, Powder Technol. 147 (2004) 94–112, https://doi.org/10.1016/j.powtec.2004.09.032.
[4] F. Cheng, Y. Feng, Q. Su, D. Wei, B. Wang, Y. Huang, Practical strategy to produce ultrafine ceramic glaze: introducing a polycarboxylate grinding aid to the grinding process, Adv. Powder Technol. 30 (2019) 1655–1663, https://doi.org/10.1016/j.apt.2019.05.014.
[5] V. Chipakwe, P. Semsari, T. Karlkvist, J. Rosenkranz, S.C. Chelgani, A critical review on the mechanisms of chemical additives used in grinding and their effects on the downstream processes, J. Mater. Res. Technol. 9 (2020) 8148–8162, https://doi.org/10.1016/j.jmrt.2020.05.080.
[6] P. Prziwara, A. Kwade, Grinding aids for dry fine grinding processes – Part I: Mechanism of action and lab-scale grinding, Powder Technol. 375 (2020) 146–160, https://doi.org/10.1016/j.powtec.2020.07.038.
[7] V. Chipakwe, T. Karlkvist, J. Rosenkranz, S.C. Chelgani, Beneficial effects of a polysaccharide-based grinding aid on magnetite flotation: a green approach, Sci. Rep. 12 (2022) 1–13, https://doi.org/10.1038/s41598-022-10304-x.
[8] V. Chipakwe, P. Semsari, T. Karlkvist, J. Rosenkranz, S.C. Chelgani, A comparative study on the e ff ect of chemical additives on dry grinding of magnetite ore, South African, J Chem. Eng. 34 (2020) 135–141, https://doi.org/10.1016/j.sajce.2020.07.011.
[9] K. Ohenoja, S. Breitung-Faes, P. Kinnunen, M. Illikainen, J. Saari, A. Kwade, J. Niinimäki, Ultrafine grinding of limestone with sodium polyacrylates as additives in ordinary portland cement mortar, Chem. Eng. Technol. 37 (2014) 787–794, https://doi.org/10.1002/ceat.201300707.
[10] P. Prziwara, S. Breitung-Faes, A. Kwade, Impact of grinding aids on dry grinding performance, bulk properties and surface energy, Adv. Powder Technol. 29 (2018) 416–425, https://doi.org/10.1016/j.apt.2017.11.029.
[11] S. Chelgani, M. Parian, P.S. Parapari, Y. Ghorbani, J. Rosenkranz, A comparative study on the effects of dry and wet grinding on mineral flotation separation–a review, J. Mater. Res. Technol. (2019) 1–8, https://doi.org/10.1016/j.jmrt.2019.07.053.
[12] P. Bulejko, N. Šuleková, J. Vlasák, R. Tuunila, T. Kinnarinen, T. Svěrák, A. Häkkinen, Ultrafine wet grinding of corundum in the presence of triethanolamine, Powder Technol. 395 (2022) 556–561, https://doi.org/10.1016/j.powtec.2021.09.079.
[13] S. Grano, The critical importance of the grinding environment on fine particle recovery in flotation, Miner. Eng. 22 (2009) 386–394, https://doi.org/10.1016/j.mineng.2008.10.008.
[14] Z. Tong, L. Liu, Z. Yuan, J. Liu, J. Lu, L. Li, The effect of comminution on surface roughness and wettability of graphite particles and their relation with flotation, Miner. Eng. 169 (2021) 106959, https://doi.org/10.1016/j.mineng.2021.106959.
[15] W.J. Bruckard, G.J. Sparrow, J.T. Woodcock, A review of the effects of the grinding environment on the flotation of copper sulphides, Int. J. Miner. Process. 100 (2011) 1–13, https://doi.org/10.1016/j.minpro.2011.04.001.
[16] O. Ersoy, D. Güler, M. Rençberoğlu, Effects of grinding aids used in grinding calcium carbonate (CACO3) filler on the properties of water-based interior paints, Coatings 12 (2022), https://doi.org/10.3390/coatings12010044.
[17] Y. Liu, G. Huang, Z. Pan, Y. Wang, G. Li, Synthesis of sodium polyacrylate copolymers as water-based dispersants for wet ultrafine grinding of cobalt aluminate particles, Colloids Surf. A Physicochem. Eng. Asp. 610 (2021) 125553, https://doi.org/10.1016/j.colsurfa.2020.125553.
[18] B. Yang, J. Liu, L. Wang, G. Ai, S. Ren, Enhanced collection of chalcopyrite by styrene-butyl acrylate polymer nanospheres in the presence of serpentine, Colloids

Surf. A Physicochem. Eng. Asp. 640 (2022) 128408, https://doi.org/10.1016/j.colsurfa.2022.128408.
[19] E. Kapeluszna, Ł. Kotwica, The effect of various grinding aids on the properties of cement and its compatibility with acrylate-based superplasticizer, Materials (Basel). 15 (2022), https://doi.org/10.3390/ma15020614.
[20] M. Lapointe, B. Barbeau, Understanding the roles and characterizing the intrinsic properties of synthetic vs. natural polymers to improve clarification through interparticle Bridging: a review, Sep. Purif. Technol. 231 (2020) 115893, https://doi.org/10.1016/j.seppur.2019.115893.
[21] C. Zhang, Y. Hu, W. Sun, J. Zhai, Z. Yin, Q. Guan, The effect of polyacrylic acid on the surface properties of calcite and fluorite aiming at their selective flotation, Physicochem. Probl. Miner. Process. 54 (2017) 868–877, https://doi.org/10.5277/ppmp1888.
[22] M. Ataie, K. Sutherland, L. Pakzad, P. Fatehi, Experimental and modeling analysis of lignin derived polymer in flocculating aluminium oxide particles, Sep. Purif. Technol. 247 (2020) 116944, https://doi.org/10.1016/j.seppur.2020.116944.
[23] M. He, Y. Wang, E. Forssberg, Parameter studies on the rheology of limestone slurries, Int. J. Miner. Process. 78 (2006) 63–77, https://doi.org/10.1016/j.minpro.2005.07.006.
[24] G.R. Quezada, E. Piceros, P. Robles, C. Moraga, E. Gálvez, S. Nieto, R.I. Jeldres, Polyacrylic acid to improve flotation tailings management: Understanding the chemical interactions through molecular dynamics, Metals (Basel). 11 (2021), https://doi.org/10.3390/met11060987.
[25] Z. Chen, Y. Wang, L. Luo, T. Peng, F. Guo, M. Zheng, Enhancing flotation separation of chalcopyrite and magnesium silicate minerals by surface synergism between PAAS and GA, Sci. Rep. 11 (2021) 1–16, https://doi.org/10.1038/s41598-021-85984-y.
[26] S. Zhang, Z. Huang, H. Wang, R. Liu, C. Cheng, S. Shuai, Y. Hu, Z. Guo, X. Yu, G. He, W. Fu, Flotation performance of a novel Gemini collector for kaolinite at low temperature, Int. J. Min. Sci. Technol. 31 (2021) 1145–1152, https://doi.org/10.1016/j.ijmst.2021.09.001.
[27] S. Shuai, Z. Huang, V.E. Burov, V.Z. Poilov, F. Li, H. Wang, R. Liu, S. Zhang, C. Cheng, W. Li, X. Yu, G. He, W. Fu, Selective separation of wolframite from calcite by froth flotation using a novel amidoxime surfactant: adsorption mechanism and DFT calculation, Miner. Eng. 185 (2022) 107716, https://doi.org/10.1016/j.mineng.2022.107716.
[28] Z. Huang, S. Shuai, V.E. Burov, V.Z. Poilov, F. Li, H. Wang, R. Liu, S. Zhang, C. Cheng, W. Li, X. Yu, G. He, W. Fu, Application of a new amidoxime surfactant in flotation separation of scheelite and calcite: adsorption mechanism and DFT calculation, J. Mol. Liq. 364 (2022) 120036, https://doi.org/10.1016/j.molliq.2022.120036.
[29] D. Mesa, P.R. Brito-Parada, Scale-up in froth flotation: a state-of-the-art review, Sep. Purif. Technol. 210 (2019) 950–962, https://doi.org/10.1016/j.seppur.2018.08.076.
[30] K. Sun, C.V. Nguyen, N.N. Nguyen, A.V. Nguyen, Flotation surface chemistry of water-soluble salt minerals : from experimental results to new perspectives, Adv. Colloid Interface Sci. 309 (2022) 102775, https://doi.org/10.1016/j.cis.2022.102775.
[31] L. Xie, J. Wang, Q. Lu, W. Hu, D. Yang, C. Qiao, X. Peng, Q. Peng, T. Wang, W. Sun, Q. Liu, H. Zhang, H. Zeng, Surface interaction mechanisms in mineral flotation: fundamentals, measurements, and perspectives, Adv. Colloid Interface Sci. 295 (2021) 102491, https://doi.org/10.1016/j.cis.2021.102491.
[32] P. Somasundaran, L.T. Lee, Polymer-surfactant interactions in flotation of quartz, Sep. Sci. Technol. 16 (1981) 1475–1490, https://doi.org/10.1080/01496398108058312.
[33] M. Hennemann, M. Gastl, T. Becker, Influence of particle size uniformity on the filter cake resistance of physically and chemically modified fine particles, Sep. Purif. Technol. 272 (2021) 118966, https://doi.org/10.1016/j.seppur.2021.118966.
[34] H. Choi, J. Lee, H. Hong, J. Gu, J. Lee, H. Yoon, J. Choi, Y. Jeong, J. Song, M. Kim, B. Ochirkhuyag, New evaluation method for the kinetic analysis of the grinding rate constant via the uniformity of particle size distribution during a grinding process, Powder Technol. 247 (2013) 44–46, https://doi.org/10.1016/j.powtec.2013.06.031.
[35] F.C. Bond, Crushing and grinding calculations, Br. Chem. Eng. 378–385 (1961).
[36] M.J. Jaycock, G.D. Parfitt, The study of liquid interfaces, Chem. Interfaces. (1981) 38–132.
[37] M. Fan, D. Tao, R. Honaker, Z. Luo, Nanobubble generation and its applications in froth flotation (part II): fundamental study and theoretical analysis, Min. Sci. Technol. 20 (2010) 159–177, https://doi.org/10.1016/S1674-5264(09)60179-4.
[38] V. Chipakwe, R. Jolsterå, S.C. Chelgani, Nanobubble-assisted flotation of apatite tailings: insights on beneficiation options, ACS Omega. (2021), https://doi.org/10.1021/acsomega.1c01551.
[39] A. Bastrzyk, J. Feder-Kubis, Pyrrolidinium and morpholinium ionic liquids as a novel effective destabilising agent of mineral suspension, Colloids Surf. A Physicochem. Eng. Asp. 557 (2018) 58–65, https://doi.org/10.1016/j.colsurfa.2018.05.002.
[40] C. Zhang, S. Wei, Y. Hu, H. Tang, J. Gao, Z. Yin, Q. Guan, Selective adsorption of tannic acid on calcite and implications for separation of fluorite minerals, J. Colloid Interface Sci. 512 (2018) 55–63, https://doi.org/10.1016/j.jcis.2017.10.043.
[41] S. Cayirli, Analysis of grinding aid performance effects on dry fine milling of calcite, Adv. Powder Technol. 33 (2022) 103446, https://doi.org/10.1016/j.apt.2022.103446.
[42] N.A. Toprak, O. Altun, A.H. Benzer, The effects of grinding aids on modelling of air classification of cement, Constr. Build. Mater. 160 (2018) 564–573, https://doi.org/10.1016/j.conbuildmat.2017.11.088.
[43] H.S. Gokcen, S. Cayirli, Y. Ucbas, K. Kayaci, The effect of grinding aids on dry micro fine grinding of feldspar, Int. J. Miner. Process. 136 (2015) 42–44, https://doi.org/10.1016/j.minpro.2014.10.001.
[44] D.W. Fuerstenau, Grinding Aids, KONA Powder Part. J. 13 (0) (1995) 5–18.
[45] V. Chipakwe, C. Hulme-Smith, T. Karlkvist, J. Rosenkranz, S.C. Chelgani, Effects of chemical additives on rheological properties of dry ground ore – a comparative study, Miner. Process. Extr. Metall. Rev. 00 (2021) 1–10, https://doi.org/10.1080/08827508.2021.1890591.
[46] M.M. Ahmed, Effect of comminution on particle shape and surface roughness and their relation to flotation process, Int. J. Miner. Process. 94 (2010) 180–191, https://doi.org/10.1016/j.minpro.2010.02.007.
[47] P. Semsari Parapari, M. Parian, J. Rosenkranz, Breakage process of mineral processing comminution machines – an approach to liberation, Adv. Powder Technol. 31 (2020) 3669–3685, https://doi.org/10.1016/j.apt.2020.08.005.
[48] A. Tohry, R. Dehghan, H. Mohammadi-Manesh, L. de S.L. Filho, S.C. Chelgani, Effect of ether mono amine collector on the cationic flotation of micaceous minerals—a comparative study, Sustain. 13 (2021) 1–13. doi:10.3390/su131911066.
[49] A.M. Vieira, A.E.C. Peres, The effect of amine type, pH, and size range in the flotation of quartz, Miner. Eng. 20 (2007) 1008–1013, https://doi.org/10.1016/j.mineng.2007.03.013.
[50] L. Wu, Y. Huang, Z. Wang, L. Liu, Interaction and dispersion stability of alumina suspension with PAA in N, N′-dimethylformamide, J. Eur. Ceram. Soc. 30 (2010) 1327–1333, https://doi.org/10.1016/j.jeurceramsoc.2009.12.010.
[51] X. Liu, J. Xie, G. Huang, C. Li, Low-temperature performance of cationic collector undecyl propyl ether amine for ilmenite flotation, Miner. Eng. 114 (2017) 50–56, https://doi.org/10.1016/j.mineng.2017.09.005.
[52] Z. Huang, H. Zhong, S. Wang, L. Xia, W. Zou, G. Liu, Investigations on reverse cationic flotation of iron ore by using a Gemini surfactant: Ethane-1,2-bis (dimethyl-dodecyl-ammonium bromide), Chem. Eng. J. 257 (2014) 218–228, https://doi.org/10.1016/j.cej.2014.07.057.
[53] W. Liu, W. Liu, X. Wang, D. Wei, B. Wang, Utilization of novel surfactant N-dodecyl-isopropanolamine as collector for efficient separation of quartz from hematite, Sep. Purif. Technol. 162 (2016) 188–194, https://doi.org/10.1016/j.seppur.2016.02.033.
[54] M. Zhu, Q. Zhang, X. Xiao, B. Shi, A novel strategy for enhancing comprehensive properties of polyacrylate coating: incorporation of highly dispersed zinc ions by using polyacrylic acid as carrier, Prog. Org. Coatings. 162 (2022) 106596, https://doi.org/10.1016/j.porgcoat.2021.106596.